2020 17th International Conference on Electrical Engineering, Computing Science and Automatic Control (CCE)
Mexico City, Mexico. November 11-13, 2020

On Balanced Tradeoffs between Stiffness and Design Area in CMOS-MEMS Accelerometer Springs

Benito Granados-Rojas, Mario Alfredo Reyes-Barranca, Luis Martin Flores-Nava
Department of Electrical Engineering – CINVESTAV, Mexico City, Mexico
e-mail: {bgranadosr, mreyes, lmflores} @cinvestav.mx

Griselda Stephany Abarca-Jiménez, Miguel Ángel Aleman-Arce, Yesenia Eleonor González-Navarro
Instituto Politécnico Nacional, Mexico City, Mexico
e-mail: {gabarcaj, maleman, ygonzalezn} @ipn.mx

Abstract – This work shows the application of an evolutionary algorithm to find a balanced tradeoff between the design area occupied by the layout of a metal folded beam spring and its stiffness, in CMOS-MEMS inertial sensor developments.

CMOS-MEMS is the set of techniques aiming to integrate micro-electromechanical structures with a variety of purposes ranging from purely capacitive to thermal and radiation-sensitive applications within the metal and semiconductor layers found in most CMOS standard fabrication processes. This integration allows to create monolithic systems where transducers and signal processing stages coexist.

The algorithm used to analyze the mentioned relations can be characterized as a genetic algorithm with three variables and two objectives functions, since these two objective (goals) are in conflict, the acquisition and discussion of results will be driven by the Pareto Optimality criteria. The solutions given by the execution of the algorithm may be taken as a start point to fine-tune the final design according to the designer preferences.

Keywords – CMOS-MEMS, MEMS, Inertial Sensor, Stiffness, Genetic Algorithm, EMOO.

I. FOLDED BEAM SPRINGS IN MEMS

The typical capacitive MEMS inertial sensor (Fig. 1) transduces the acceleration produced by gravity or external applied forces to a proportional change in the capacitance of a varactor which is usually conformed by two sets of interleaved metallic beams or plates, one of them fixed and one movable, suspended by two or more also metallic springs. Most of these designs include a bulky plate that performs as a relatively significant mass and makes the device more sensitive to acceleration.

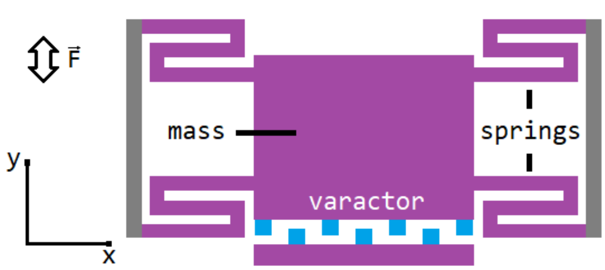

Fig. 1. Typical MEMS capacitive structure for inertial sensors.

This mechanical structure can be fairly well described as a simple mass-spring system. Where in terms of the Hooke's Law (1), the displacement Δy and therefore, the capacitance are proportional to the applied force F and to the inverse of the equivalent stiffness k of the spring system. While being mechanically connected in a parallel configuration, the equivalent stiffness (2) is equal to the sum of all the individual contribution of each spring.

$$\Delta y = \frac{F}{k_{eq}} = \frac{m_{pm}a}{k_{eq}} \tag{1}$$

$$k_{eq} = \Sigma k_i \tag{2}$$

Many springs used for the suspension of the proof mass in MEMS sensors [1][2][3] consists in oblong beams with one or more folds. Stiffness in cantilever beams determines how much the free end displaces when a load is applied, for a beam with a given rectangular section area stiffness (3) is given by the moment of inertia I of the section (in terms of the width of the base b, the height h), the length l of the beam itself, and the Young's Modulus E of the material. For the case of typical MEMS, the height parameter corresponds with the thickness t_M of the metal layer and width b and length l are the dimensions W_b and L_b for the beam respectively as drawn in the layout from a top view. So, in CMOS-MEMS technology, the stiffness for a single beam spring reacting to an applied force in the y-axis direction is given by expression (4).

$$k = \frac{3EI}{l^3} = \frac{3E}{l^3}\frac{b^3h}{12} \tag{3}$$

$$k = \frac{Et_M}{4}\left(\frac{W}{L}\right)^3 \tag{4}$$

Although the modeling and simulation of stiffness and other mechanical properties in this work are based in an aluminum structure (with $E = 70\text{GPa}$), MEMS designers must be aware of the true composition of metal layers in different CMOS fabrication processes. As seen in [4], the C5 process by On-Semi has three metal layers, every of them consisting in an interior aluminum sheet with top and bottom covers of titanium nitride (TiN) what gives superior contact and mechanical strength capabilities, but also negatively affects the wet etch post-processing needed to the CMOS to CMOS-MEMS conversion.

II. THE OBJECTIVE FUNCTIONS

The effective stiffness along with the design area are two mayor concerns when it comes to MEMS spring design. The first is what makes an inertial sensor device more or less appropriate for low-G or high-G application i.e. a seismometer in contrast to an industrial centrifuge or vibration meter.

Models in the present work are quite simple due to their nature and reduced number of parameters. They are an example of a two-objective optimization problem since they are effectively in conflict. As from equation (4) stiffness (desired to be lower in most applications) decreases as the W/L ratio does so, but once the inferior limit for W is reached (having a very narrow wire) the only option is continuing to reduce the length of the beam L. When having a single beam spring, the area consumed by the structure is simply $A = WL$, but for two or more segments array (Fig. 2), and having a simplification to a uniform same-width wire (and square $W \times W$ joints), the area of spring is given by (5) where n is the number of segments.

$$A = (2n - 1)WL \tag{5}$$

Stiffness (6) in the other hand, decreases proportionally to the number beams as they are connected in a mechanical series configuration.

$$k = \frac{1}{n}\frac{Et_M}{4}\left(\frac{W}{L}\right)^3 \tag{6}$$

Both models have the very same three variable parameters n, W, and L and both are intended to be minimized, what makes the problem suitable to try to find a reasonable stiffness to area ratio by means of metaheuristic procedures, determining the possible "best" solution according to criteria of the Pareto Optimality [5].

III. GENETIC ALGORITHM

Genetic algorithms are considered bio-inspired metaheuristics, due to common base they have of approach computationally the behavior and evolution of a group of individual that across many generations (epochs) recombine their genetic information in order to create more capable individuals meeting better the overall goals of the population.

Fig. 2. Variable parameters.

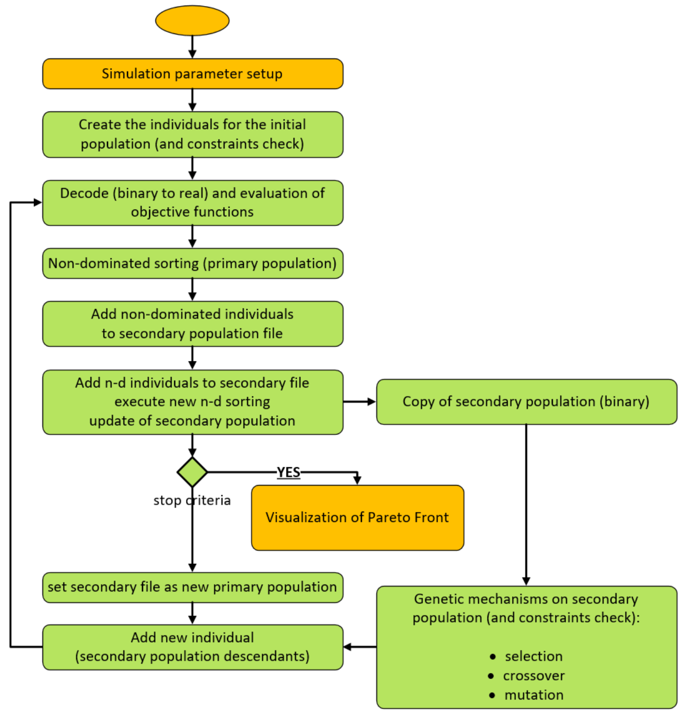

Fig. 3. Bio-inspired metaheuristic algorithm.

Fig. 3 summarizes the stages and procedures that take place during the evolution of a representative population. Each individual of the population is unique and its genetic data corresponds to a feasible solution of the engineering problem, this is, the so called chromosome is a codified collection of bits where the number of variables in the problem determines the number of genes that concatenate in a single, usually binary, bit string. A particular bit string can be decoded into a particular configuration of numerical values for each variable and by evaluating the objective functions with the decoded data we obtain the specific *fitness* value for the given individual. The codification of variables is summarized in Table 1 in terms of multiples of the minimum CMOS layout feature λ.

var	range	min	max	bits
L	$100 - 1000\lambda$	30µm	300µm	5
W	$10 - 100\lambda$	3µm	30µm	4
n	$5 - 15$	5 beams	25 beams	4
Total chromosome length				19

Table 1. Variables codification.

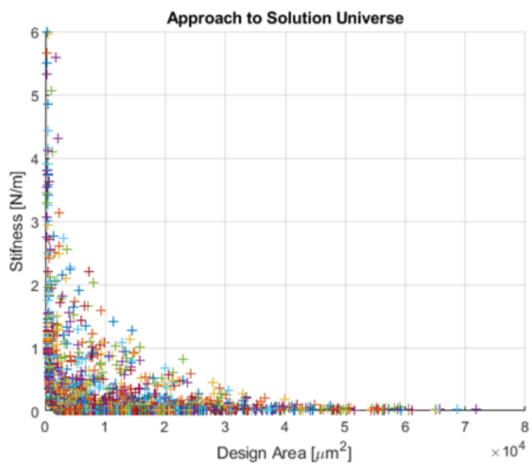

Fig. 4. Approach to the shape of the search space (a projection to the objective-function space).

The initial population in the simulation is random-like generated not without a constraint filtering. Since a full random individual might represent a not feasible (not compatible with the fabrication processes nor design rules) solution for the problem these individuals must be suppressed before they recombine with other, spreading their characteristics. An example of constraint is to keep an aspect ratio for the beams being L greater than ten times the value of W. Figure 4 shows an approach to the shape of the search space for all possible individuals (solutions, configurations) in a two-beam design that already cleared the constraints check. However, this is a projection in the two-dimensional space of the objective functions, the actual search space corresponds to a cube in the three-dimensional space within the limits of variables L, W, and n. More detailed (and realistic) models for each objective function would lead to a search space on higher dimensions.

III. SIMULATION AND RESULTS

The algorithm described above was implemented a total of six times, ten runs each, with different population parameters and restrictions, as summarized in Table 2, the first set of four executions had variation in the population and generation parameters while letting the form factor (aspect ratio) of the whole spring (not only of each beam) free. The last two simulation added restrictions in the form factor of the spring to meet a particular width to length ratio.

set	runs	generations	pop. size	additional constraints
A	10	10	1000	-
B	10	50	1000	-
C	10	10	5000	-
D	10	50	5000	-
E	10	10	3000	$(2n-1)W/L \geq 0.5$
F	10	10	10	$(2n-1)W/L \geq 0.9$

Table 2. Summary of algorithm execution parameters.

Each one of the executions of the algorithms give us information about the Pareto Front for the two-objective problem, the Pareto Front is the collection of non-dominated solutions after having decoded every individual, evaluated the objective functions and performed a non-dominated sorting among the current population. A non-dominated solution is one so that there is no other solution better fitted to both objectives at the same time. Pairs of non-dominated individuals are selected from current and previous generations, stored in a secondary repository file (and updated with a new sorting each generation) and then recombined into new ones with intermediate characteristics to create the next generation and so on until meeting an stop criteria. Figure 5 depicts a Pareto Front for a two-beam spring design (set D) zoomed in to the knee region where the stiffness-area tradeoff is closer to an idealistic solution (where both objectives are minimized). The dashed line runs from the idealistic solution to the closest one in the Pareto Front, this calculation is made by normalizing both objective within their minimum and maximum values and then measuring the Euclidean distance to every solution. As can be seen in Table 3, a set of runs with higher population is likely to retrieve more points in the Pareto Front (non-dominated solutions). Results from set D to F where further processed and validated via multi-physics simulation software with finite element analysis.

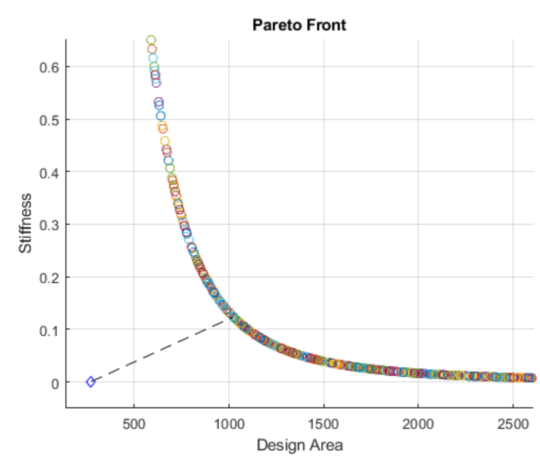

Fig. 5. Knee region in a typical Pareto Front.

set	L (µm)	W (µm)	n	A (µm^2)	k (N/m)	nd-sols
A	121.2	3	2	1090.8	0.1021	369
B	113.4	3	2	1020.6	0.1247	299
C	113.7	3	2	1023.3	0.1237	781
D	113.7	3	2	1023.3	0.1237	769
E	64.5	3	6	2128.5	0.2259	275
F	63.0	3	10	3591.0	0.1455	125

Table 3. Summary of algorithm execution results.

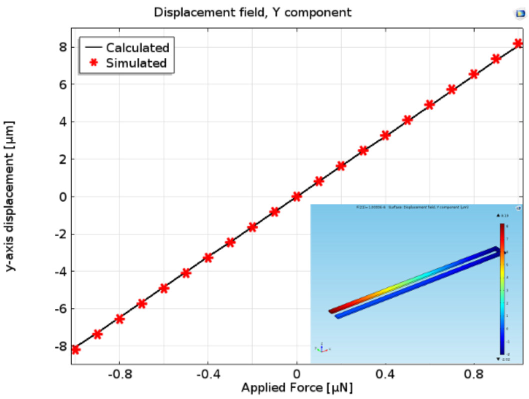

a.

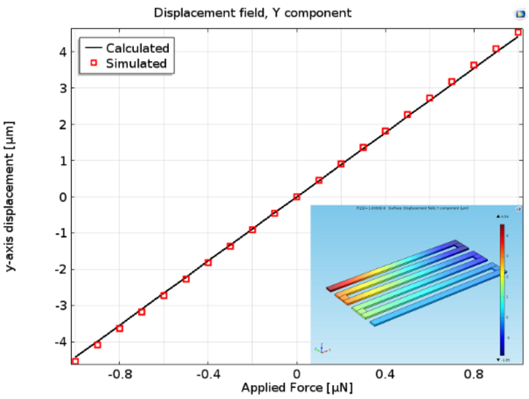

b.

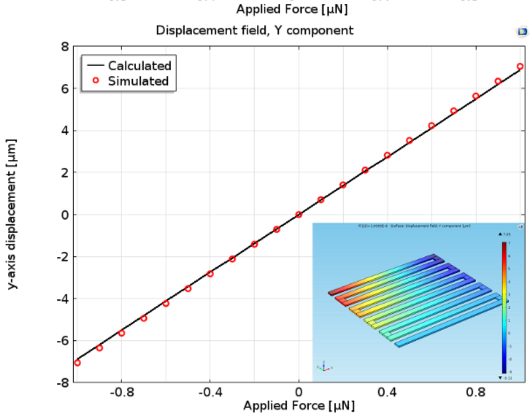

c.

Fig. 6. Validation of stiffness according to solutions from the algorithm for (a) set D, (b) set E, and (c) set F.

As for Table 3, it is evident that W and n tend to their minimum possible value, while the predominant variable is length L, but this is not necessarily true for every specific design goal since W value is mainly driven by the stiffness goal while increasing n affects more directly to the area objective function. The data obtained from the knee region of the Pareto Front must be interpreted as a balanced tradeoff between the two or more goals for a given problem, the selected solution (the closest to the idealistic point) is one with a fitness for both stiffness and area design relatively good at the same time. Figure 6 shows the validation of the stiffness by comparing the *simulated* behavior of a 3D model in FEA software for 2-, 6-, and 10-beam spring and the *calculated* (estimation with the values drew by the genetic algorithm).

IV. CONCLUSIONS

The multi-physical and multi-criteria nature of CMOS-MEMS devices make them suitable to try a variety of bio-inspired metaheuristic methods. The pertinence of using such techniques must be pondered by the layout designer yet being an automation to the first design stages that serves as a source of initial optimal or near-to-the-optimal parameters from which fine adjustments can be made to reach the ultimate design goals.

This study case successfully reports what must be expected when applying the metaheuristic to a quite simple, purely mechanical yet very common design problem within the framework of microelectronics, challenges such as model longer bonds (non-square) between beams inclusion of external forces, temperature, etc. may require more sophisticated analysis in the conceptualization and implementation of objective function and constraints handle.

The modeling and test of these mechanical subsystems is intended to be extended in such a way that a single algorithm will be capable perform full or partial automation of the design of MEMS devices integrating electromechanical transduces along with both analog and digital electronics.

V. FUTURE WORK

As discussed above, a genetic algorithm and some others in the family of the EMOO acquires relevance with larger problems, this kind of algorithm is intended to be used in a similar problem with a more sophisticated modeling of the objective functions, including but not limited to the addition of gravitational effects, compound materials in the metal layers and irregular geometries in the topology of layouts.

ACKNOWLEDGMENTS

We would like to thank to the National Council of Science and Technology (CONACYT) and the VLSI Lab's community for the resources and advices given during the development of the present work.

REFERENCES

[1] Karbari, Sudha & Kumari, Uttara & Pasha C, Roshan & K Gowda, Vikas. (2018). Design and analysis of serpentine based MEMS accelerometer. AIP Conference Proceedings.

[2] Lin, Chun-Ying & Chiou, Jin Chern. (2012). MEMS-based thermally-actuated image stabilizer for cellular phone camera. Journal of Micromechanics and Microengineering.

[3] Park, Byoungyoul & Afsharipour, Elnaz & Chrusch, Dwayne & Shafai, Cyrus & Andersen, David & Burley, Greg. (2017). Large Displacement Bi-Directional Out-of-Plane Lorentz Actuator Array for Surface Manipulation. Journal of Micromechanics and Microengineering.

[4] B. Granados-Rojas, M. A. Reyes-Barranca, et al. "3-layered Capacitive Structure Design for MEMS Inertial Sensing." 2016 13th International Conference on Electrical Engineering, Computing Science and Automatic Control (CCE). 2016

[5] Censor, Y. Pareto optimality in multiobjective problems. Appl Math Optim 4, 41–59 (1977).